Nonlinear control of friction-induced limit cycle oscillations via feedback linearization

L. Nechak

Nonlinear Control of Friction-induced Limit Cycle Oscillations via Feedback Linearization

L. Nechak[a]

[a] *Laboratoire de Tribologie et Dynamique des Systèmes, UMR CNRS 5513, École Centrale de Lyon, 36 avenue Guy de Collongue 69134 Écully Cedex, France (e-mail: lyes.nechak@ec-lyon.fr).*

Abstract

This paper deals with the active control of friction-induced limit cycle oscillations that are generated from the mode-coupling mechanism, and that are often undesirable in numerous applications of nonlinear dynamical friction systems. The objective is to suppress the oscillations while taking into account the nonlinearities inherent to the friction systems and that result for example from the nonlinear laws of contact and friction. For this purpose, nonlinear control schemes based on the feedback linearizing approach are proposed and investigated in this study by considering a friction system with mode-coupling instabilities. Based on numerical simulations, an interesting potential is shown for the proposed control schemes and, more generally, insights about the opportunity to exploit them for an efficient mitigating of mode coupling instabilities, are stated.

Keywords: Nonlinear dynamical systems, Friction-induced instabilities, mode-coupling, Nonlinear control, Feedback linearization, Flatness, Stability.

1. Introduction

In numerous engineering applications, friction-induced instabilities are in general undesirable due to their negative effects on systems performances. Brake squeal is a well known example in this area ([1, 2]). Hence, numerous studies have been carried out for a better understanding of mechanisms of their occurrences [3, 4]. Other studies have focused on the developing of methods helping for efficient prediction of friction-induced instabilities and their properties in deterministic framework, such as in [5, 6, 7, 8] and in uncertain context as in [9, 10, 11, 12, 13, 14]. In addition to the need to be able to effectively model and predict friction-induced instabilities, a very important purpose is

to be capable of mitigating or suppressing them if it turns out that the vibratory level is unacceptable. This last issue is the key topic of the present study.

In fact, a number of studies have been proposed these last years for the controlling of friction-induced instabilities. For example, Bergeot et.al have proposed a passive control strategy based on Nonlinear Energy Sink (NES) [15]. The main developed idea consists of adding a mass-stiffness-damping cell with some nonlinear properties, to the initial unstable system. The key step is then to determine the mechanical parameters of the NES so that the controlled system presents suitable stability properties and a fortiori convenient dynamic behaviour. The authors have shown that the NES parameters can be tuned for either a complete suppression or a mitigating of the original amplitude of the friction-induced limit cycle oscillation (LCO). In the same register of passive control, Popp and Rudolph have proposed the use of a dynamic vibration absorber to control the friction-induced instabilities related to stick-slip mechanisms [16]. They have shown that by determining a suitable set of parameters, the absorber can prevent or minimize the amplitude of the stick-slip based limit cycle oscillations. Otherwise, Ouyang has proposed structural modifications for an unstable friction system and has shown that this strategy is not always suitable for assigning eigenvalues to the desired locations and thus for stabilizing the system [17]. Active control strategies based on linear state feedback [18] and on linear delayed state feedback [19, 20, 21, 22] were proposed as alternative for controlling friction-induced instabilities. The main principle of these schemes is to act on all the system eigenvalues by assigning them to desired locations in the half left complex plane so that stable dynamic behaviours can be ensured. In the case of systems with high numbers of degrees of freedom, this task can be very difficult and some times unnecessary. To circumvent this difficulty, a linear state feedback which permits a partial pole assignment in systems submitted to friction-induced instabilities was proposed in [23].

Dealing with the control of friction-induced vibrations submitted to parameter uncertainty was the objective of the recent study in [24]. The main treated question concerns how to robustly stabilize a linear mechanical system submitted to friction-induced instabilities with respect to the uncertainty related to the contact and friction parameters. Authors have proposed a robust linear state feedback assigning both eigenvalues and their

sensitivities to desired locations and values respectively. The proposed control scheme ensures a maximum degree for the robustness of the stability of the closed loop system with respect the considered uncertain parameters.

Most of the mentioned studies have proposed linear techniques for active control of friction-induced instabilities. However, these instabilities are often the consequence of the contact with friction between structures and the laws governing the contact and friction may be strongly nonlinear. Hence, linear schemes may be unsuitable and/or insufficient for an efficient and reliable control of friction-induced instabilities and nonlinear control schemes become more appropriate. This paper focuses on this issue. Otherwise, problems related to practical implementation of the control input such as the saturation problem and its robustness with respect to parameter uncertainty and/or unmodeled dynamics are not considered in this paper. Some effective solutions related to these issues are discussed for example in [25] within the framework of controlling of double-pendulum cranes. Then, the main contribution of the proposed study lies in the taking into account of nonlinearities in the defining of active control schemes for more efficient mitigating of nonlinear friction-induced vibrations in particular those generated from the mode-coupling mechanism. The latter occurs when a couple of complex eigenvalues approach one another in frequency when the friction coefficient increases until coalescence at the Hopf bifurcation point around which the corresponding real parts separate. When at least one real part becomes positive, self-friction-induced vibrations can be generated [3, 4]. The main problem is then to mitigate or suppress these vibrations. As stated above, only passive control based strategies have been proposed to deal with this issue while the mentioned active control strategies are based on linear schemes that are not suitable candidates for efficient control of nonlinear mode-coupling instabilities. Hence, methods based on nonlinear feedback linearization [26, 27] are proposed and investigated in this paper. The main objective is to assess their efficiency in dealing with the mitigating of nonlinear mode-coupling instabilities.

In fact, the feedback linearization principle considers the possibility to determine a nonlinear coordinate transformation which algebraically puts the nonlinear system into a canonical form based on which the choosing of a suitable state feedback makes the system partially or completely linear. The latter is then said input-output or input-state lin-

earized, respectively. At this stage, the use of linear control techniques becomes possible. The input-state linearization is always possible when the system presents some flatness properties which consist in the possibility to express all the system' inputs and state variables by means of the system'output and its successive derivatives [28]. The relative degree of the input-output relation, which is the number of required output derivative to make the input appear, is in this case equal to the system' dimension. The control synthesis is then reduced to a classical pole placement problem [26, 27, 29]. Otherwise, the input-output linearization holds when the relative degree is smaller than the system' dimension. In this case, a linear relation between the input and output is obtained while the input-state relation defining the internal dynamics remains nonlinear. The stabilizing problem possesses a solution when the internal dynamics which is uncontrolable is stable [26, 27].

The linearizing feedback techniques have already been proposed to deal with numerous problems in engineering such as the output tracking control design for an helicopter model [30], the control of aeronautic pneumatic systems [31] and the control for the anti-slip regulation of an hybrid vehicle [32]. New theoretical developments are also proposed in the recent study [33]. They are based on the combination between the receptance method well known in LTI systems together with the input-output linearizing feedback. The main contribution of the resulting method makes the system matrices (with associated assumptions and approximations) unnecessary to be known. Moreover, the form and parameter values of the nonlinearity are not required when the force is applied at the same degrees of freedom as the input and output while it does not act directly on the nonlinearity itself.

Both the input-output and input-state linearizing feedbacks are considered and investigated in this study the originality of which is, as mentioned previously, related to the mitigating of mode-coupling instabilities by taking into account of their nonlinear character. More particularly, it aims to investigate the effectiveness of the feedback linearization based methods and to obtain insight about the opportunity to use them for active control of nonlinear friction systems submitted to mode-coupling instabilities.

This paper is organized as follows. First, some mathematical notions related to nonlinear dynamical systems is given in Section 2. The feedback linearization principle

is then described in Section 3 while its application for the controlling of friction-induced mode-coupling instabilities is presented and discussed in Section 4. Conclusion is given at the end of the paper.

2. Nonlinear dynamical systems and methematical background

Consider the class of single-input/single output (SISO) nonlinear dynamical system affine with respect to the input u, and described by the following state space representation:

$$\dot{\boldsymbol{x}} = \boldsymbol{f}(\boldsymbol{x}) + \boldsymbol{g}(\boldsymbol{x})u \tag{1}$$

where $\boldsymbol{f} : R^n \rightarrow R^n$ is a smooth nonlinear vector field, involving the existence and the continuity of its partial derivatives of any required order. Then, the Jacobian matrix can be defined by $\nabla \boldsymbol{f} = \frac{\partial \boldsymbol{f}}{\partial \boldsymbol{x}}$ with element given by $(\nabla f)_{ij} = \frac{\partial f_i}{\partial x_j}$. The output of the system is given by the following output equation:

$$y = h(\boldsymbol{x}) \tag{2}$$

where h is a smooth scalar function of the state vector $\boldsymbol{x}$, with the gradient denoted by the row vector ∇h such $(\nabla h)_i = \frac{\partial h}{\partial x_i}$.
Without lose of generality, lets consider that the origin $(\boldsymbol{x}_{\mathrm{e}}, u_{\mathrm{e}}) = (\boldsymbol{0}, 0)$ is the equilibrium of System (1). The main concern in the following is to determine a state feedback control $u = \gamma(\boldsymbol{x})$ such that the closed loop system

$$\dot{\boldsymbol{x}} = \boldsymbol{f}(\boldsymbol{x}) + \boldsymbol{g}(\boldsymbol{x})\gamma(\boldsymbol{x}) \tag{3}$$

is locally asymptotically stable (the eigenvalues of the closed loop system around the equilibrium are with strictly negative real parts).
Nonlinear techniques based on linearizing feedback are proposed in the sequel in order to determine $\gamma(\boldsymbol{x})$. Some mathematical notions from the Lie algebra required for the proposed techniques are recalled from [26, 27].

Let $L_{\boldsymbol{f}}h$ be a scalar function denoting the Lie derivative of h with respect to $\boldsymbol{f}$ defined by: $L_{\boldsymbol{f}}h = \nabla h \boldsymbol{f}$. Additionally, lets denote by $[\boldsymbol{f}, \boldsymbol{g}]$ the Lie bracket of $\boldsymbol{f}$ and $\boldsymbol{g}$ which is defined by: $[\boldsymbol{f}, \boldsymbol{g}] = \nabla \boldsymbol{g} \ \ \boldsymbol{f} - \nabla \boldsymbol{f} \ \ \boldsymbol{g}$. The repeated Lie brackets are then defined

recursively by the operator ad such that:

$$\begin{cases} ad^0_{\boldsymbol{f}}\boldsymbol{g} = \boldsymbol{g} \\ \vdots \\ ad^i_{\boldsymbol{f}}\boldsymbol{g} = \left[\boldsymbol{f}, ad^{i-1}_{\boldsymbol{f}}\boldsymbol{g}\right] \end{cases} \tag{4}$$

Definition.1 (Involutive distribution of vector fields): let $\Delta = span\left\{\boldsymbol{f^1}, \boldsymbol{f^2}, ..., \boldsymbol{f^m}\right\}$ a distribution of m linearly independent vector fields. Then Δ is said involutive if the following rank condition is fulfilled:

$$\text{rank}\left(\left\{\boldsymbol{f^1}, \boldsymbol{f^2}, ..., \boldsymbol{f^m}, \left[\boldsymbol{f^i}, \boldsymbol{f^j}\right]\right\}\right) = \text{rank}\left(\left\{\boldsymbol{f^1}, \boldsymbol{f^2}, ..., \boldsymbol{f^m}, \right\}\right) \qquad \forall \{i, j\} \subset \{1, ..., m\} \tag{5}$$

where i and $j \in \{1, 2, ..., m\}$ are integers denoting the indices of the vector fields constituting the distribution.

Definition.2 (Rrelative degree): System (1) with the output equation (2) admits the scalar r as the relative degree within a region of the state space, $\Omega \subset R^n$, if r verifies the following two conditions:

$$\begin{cases} L_{\boldsymbol{g}} L^k_{\boldsymbol{f}} h(\boldsymbol{x}) = 0 & \forall k < r-1 \\ L_{\boldsymbol{g}} L^{r-1}_{\boldsymbol{f}} h(\boldsymbol{x}) \neq 0 & \forall \boldsymbol{x} \in \Omega \end{cases} \tag{6}$$

In fact, the relative degree r represents the number of successive derivatives of the output $y = h(\boldsymbol{x})$, from which the control input u appears.

3. Feedback linearization

The main idea is to determine a nonlinear coordinate transformation

$$\boldsymbol{z} = \boldsymbol{\Phi}(\boldsymbol{x}) \tag{7}$$

with $z_i = \phi_i(\boldsymbol{x}) = L^{i-1}_{\boldsymbol{f}} h(\boldsymbol{x}), i = 1, ..., r$, $L^0_{\boldsymbol{f}} h(\boldsymbol{x}) h(\boldsymbol{x}) = h(\boldsymbol{x})$

together with a nonlinear state feedback simplifying the nonlinearities of System (1) so that the closed loop system can be written in a linear form and linear control techniques can be exploited. Two cases can be distinguished according to the value of the relative degree r: the input-output linearization which corresponds to the case where $r < n$ and

the input-state linearization corresponding to the case $r = n$. In fact, the new state vector $\boldsymbol{z}$ is linked to System (1) and (3) via the nonlinear coordinate transformation $\boldsymbol{\phi}$ which, as it will presented in the following, is determined in a such a way that it is bijective (so $\boldsymbol{x} = \boldsymbol{\phi}^{-1}(\boldsymbol{z})$), by considering the output function the relative degree of which define the way to determine the transformation.

3.1. Input-Output lineatization

When the relative degree r is smaller than the system dimension n then the nonlinear coordinate transformation $\boldsymbol{z} = \boldsymbol{\Phi}(\boldsymbol{x})$ must be completed by the functions $\phi_j(\boldsymbol{x}), j = r+1, ..., n$, given by the solutions of the following equations

$$L_{\boldsymbol{g}}\phi_j(\boldsymbol{x}) = 0 \tag{8}$$

in order to define a diffeomorphism $\boldsymbol{\Phi} = \begin{bmatrix} \phi_1 & \phi_2 & \cdots & \phi_n \end{bmatrix}^{\mathrm{T}}$; $\boldsymbol{\Phi}$ is bijective (i.e. the inverse function $\boldsymbol{\Phi}^{-1}$ exists). Hence, by applying the completed nonlinear coordinate transformation together with the nonlinear state feedback defined by

$$u = \frac{1}{b(\boldsymbol{\xi}, \boldsymbol{\tau})}\left[-a(\boldsymbol{\xi}, \boldsymbol{\tau}) + v\right] \tag{9}$$

with $a(\boldsymbol{\xi}, \boldsymbol{\tau})$ and $b(\boldsymbol{\xi}, \boldsymbol{\tau})$ given by

$$\begin{cases} a(\boldsymbol{\xi}, \boldsymbol{\tau}) = L_{\boldsymbol{f}}^{r} h(\boldsymbol{\Phi}^{-1}(\boldsymbol{\xi}, \boldsymbol{\tau})) \\ b(\boldsymbol{\xi}, \boldsymbol{\tau}) = L_{\boldsymbol{g}} L_{\boldsymbol{f}}^{r-1} h(\boldsymbol{\Phi}^{-1}(\boldsymbol{\xi}, \boldsymbol{\tau})) \end{cases} \tag{10}$$

where $\boldsymbol{\xi} = \begin{bmatrix} z_1 & z_2 & \cdots & z_r \end{bmatrix}^{\mathrm{T}} = \begin{bmatrix} y & \dot{y} & \cdots & y^{r-1} \end{bmatrix}^{\mathrm{T}}$, with y and y^{r-1} being the output and its $(r-1)$-th time derivative which is equivalent to the $(r-1)$-th Lie derivative with respect to $\boldsymbol{f}$ and $\boldsymbol{\tau} = \begin{bmatrix} z_{r+1} & \cdots & z_n \end{bmatrix}^{\mathrm{T}}$,
then the original nonlinear system (1) is put into the following canonical form

$$\begin{cases} \dot{\boldsymbol{\xi}} = \boldsymbol{A}\boldsymbol{\xi} + \boldsymbol{B}v \\ y = z_1 \\ \dot{\boldsymbol{\tau}} = \boldsymbol{q}(\boldsymbol{\xi}, \boldsymbol{\tau}) \end{cases} \tag{11}$$

where $\boldsymbol{A} = \begin{bmatrix} 0 & 1 & 0 & 0 & \cdots & 0 \\ 0 & 0 & 1 & 0 & \cdots & 0 \\ \vdots & \vdots & 0 & \ldots & \ldots & \vdots \\ \vdots & \vdots & \vdots & \ldots & \ldots & 1 \\ 0 & 0 & 0 & 0 & \ldots & 0 \end{bmatrix} \in R^{r\times r}$ and $\boldsymbol{B} = \begin{bmatrix} 0 \\ 0 \\ \vdots \\ \vdots \\ 1 \end{bmatrix} \in R^{r\times 1}$

v is the new control input, $\boldsymbol{q} = \begin{bmatrix} q_{r+1} & \cdots & q_n \end{bmatrix}^{\mathrm{T}}$ with q_i are functions in the vector variables $\boldsymbol{\xi}$ and $\boldsymbol{\tau}$.

The $\boldsymbol{\xi}$ and $\boldsymbol{\tau}$ are called the normal coordinates while the closed loop system (11) is said to be input-output linearized. Two subsystems can be distinguished from (11); a r-dimensional linear system in which the control u appears and a $(n-r)$-dimensional uncontrollable nonlinear system which represents the internal dynamics. In fact, the dynamics of the closed loop system (11) presents an input-output map which consists of a linear relation between y and v, and an internal part which remains unchanged by the new control input v. However, it can be remarked that the matrix $\boldsymbol{A}$ possesses all its eigenvalues at zero, which gives rise to unstable behaviour for the closed loop system regardless the stability of the internal dynamics defined by $\dot{\boldsymbol{\tau}}$. As the linear part is controllable, then the closed loop system (11) is said to be locally asymptotically stabilizable by using a second state feedback

$$v = \boldsymbol{K}_{\mathrm{PL}}\boldsymbol{\xi} \tag{12}$$

with $\boldsymbol{K}_{\mathrm{PL}}^{\mathrm{T}} \in R^{r\times 1}$,

if and only if the internal dynamics is locally asymptotically stable. Hence in this case, the stabilizing problem comes down to a classical linear problem of pole placement [29]. However, the key step in the stabilizing procedure is to determine the stability of the internal dynamics corresponding to the last $n-r$ states in the normal form (11). Analysing this stability has been shown to be equivalent to the analysis of the zero-dynamics which corresponds to the internal dynamics when the control input is such that the output y is maintained at zero. A such control input is given by:

$$u_0(\boldsymbol{\tau}) = -\frac{a(\mathbf{0}, \boldsymbol{\tau})}{b(\mathbf{0}, \boldsymbol{\tau})} \tag{13}$$

where the $\boldsymbol{\xi}$ is constrained to zero as the output y and thus the successive derivatives are also constrained to zero [26, 27].

The stabilizing procedure based on the input-output linearizing approach can be summarized by the following algorithm.

Algorithm 1

1. Calculate the relative degree r
2. Construct the diffeomorphism $\boldsymbol{\Phi}$ by using (7) and (8)
3. Calculate the input-output linearizing feedback u given by (9) and (10)
4. Determine the stabilizing state feedback defined by (12)
5. Analyse the stability of the zero-dynamics and the whole closed loop system

3.2. Input-state linearization

The previous case has defined the input-output linearization feedback where the input-output relation is characterized by a relative degree r smaller than the system's dimension n. A complete linearization called input-state linearization can be defined for System (1) if and only if there exists a scalar function $\varphi(\boldsymbol{x})$ within a region $\Omega \in R^n$ such that the system's input-output linearization with $\varphi(\boldsymbol{x})$ as an output function has relative degree $r = n$. The existence of a such function is guaranteed if the following two conditions are fulfilled:

1. $\text{Rank}(\boldsymbol{M}_g) = n$ in Ω

   where

$$\boldsymbol{M}_g = \left(\begin{bmatrix} \boldsymbol{g} & ad_{\boldsymbol{f}}\boldsymbol{g} & \dots & ad_{\boldsymbol{f}}^{n-2}\boldsymbol{g} & ad_{\boldsymbol{f}}^{n-1}\boldsymbol{g} \end{bmatrix} \right) \tag{14}$$

2. The distribution $\bar{\Delta} = span\left\{\boldsymbol{g}, ad_{\boldsymbol{f}}\boldsymbol{g}, \dots, ad_{\boldsymbol{f}}^{n-2}\boldsymbol{g}\right\}$ is involutive in Ω.

Hence by considering the coordinate transformation $\boldsymbol{z} = \boldsymbol{\Phi}(\boldsymbol{x})$ involved by the scalar output function $\varphi(\boldsymbol{x})$ such that

$$z_i = L_{\boldsymbol{f}}^{i-1}\varphi(\boldsymbol{x}), i = 1, ..., n \tag{15}$$

, and the state feedback (9) with :

$$\begin{cases} a(\boldsymbol{z}) = -\frac{L_{\boldsymbol{f}}^{n}\varphi(\boldsymbol{\Phi}^{-1}(\boldsymbol{z}))}{L_{\boldsymbol{g}}L_{\boldsymbol{f}}^{n-1}\varphi(\boldsymbol{\phi}^{-1}(\boldsymbol{z}))} \\ b(\boldsymbol{z}) = \frac{1}{L_{\boldsymbol{g}}L_{\boldsymbol{f}}^{n-1}\varphi(\boldsymbol{\Phi}^{-1}(\boldsymbol{z}))} \end{cases} \tag{16}$$

and the new input v, System (1) is transformed into the canonical form of Brunovsky which is the well-known companion representation for the controllability [29].

$$\begin{cases} \dot{\boldsymbol{z}} = \boldsymbol{A}\boldsymbol{z} + \boldsymbol{B}v \\ y = \varphi(\boldsymbol{x}) = z_1 \end{cases} \tag{17}$$

where in this case the state, $\boldsymbol{A}$, and control, $\boldsymbol{B}$, matrices given in (11) are defined in $R^{n\times n}$ and $R^{n\times 1}$ respectively.

As in the case of input-output linearization, the obtained closed loop system is unstable since all the n eigenvalues of the state matrix $\boldsymbol{A}$ are equal to zero. Hence, a supplementary state feedback is necessary to make the closed loop system asymptotically stable. The main advantage in this case is that the couple $(\boldsymbol{A}, \boldsymbol{B})$ is controllable so the closed loop system (17) can be made asymptotically stable by solving the corresponding pole placement problem [29]. Ultimately, the stabilizing procedure based on the input-state linearizing approach can be summarized by the following algorithm.

Algorithm 2

1. Calculate $\boldsymbol{g}(\boldsymbol{x}^0), ad_{\boldsymbol{f}}\boldsymbol{g}(\boldsymbol{x}^0), \ldots, ad_{\boldsymbol{f}}^{n-1}\boldsymbol{g}(\boldsymbol{x}^0)$, $\boldsymbol{x}^0 \in \Omega$.
2. Verify the rank condition for the matrix $\boldsymbol{M}_{\mathrm{g}}$ and the involutivity of the distribution $\bar{\Delta}$.
3. Determine the output function $\varphi(\boldsymbol{x})$.
4. Construct the diffeomorphism as defined by (15).
5. Calculate the linearizing feedback (9) by using (16)
6. Determine the state feedback stabilizing the input-state linearized system (17) by solving the corresponding pole placement problem.

4. Application to the control of mode-coupling instabilities

In order to analyse the effectiveness of the proposed nonlinear techniques based on feedback linearization in the controlling of mode-coupling instabilities, a mechanical system is considered in Figure (1). It is a minimal model (two degrees of freedom) which was defined by Hultèn [34] for enhancing the understanding of the mechanisms generating instabilities in drum brake systems. In fact, the Hultèn model has been shown to be a suitable model for a faithful representation of mode-coupling instabilities occurring

in drum brake systems so, it has been considered in several other studies such as in ([35, 36]) for the analysis of the influence of damping on the mode-coupling instabilities or in ([37, 12, 38, 13]) for the prediction of mode-coupling instabilities submitted to parameter uncertainty and, more recently, for the analysis of the performances of passive control based on the NES in the mitigating of mode-coupling instabilities. Otherwise, as mentioned in the introduction of this paper, several other studies have proposed minimal models to develop and test control strategies for the mitigating of friction-induced instabilities [17, 18, 19, 24]. The main advantage of such models is that they make it possible to overcome the numerical difficulties that may be involved by the considering of high dimensional models and thus they permit to focus mainly on the methodologies. So, in this same perspective the Hultèn model is considered in the following to analyse the performances of the feedback linearization based schemes and their efficiency in dealing with the controlling of LCO generated from mode-coupling mechanisms.

[Figure 1 about here.]

As illustrated in Figure (1), the mechanical system consists in a mass assumed to be in a permanent contact with a moving band. The contacts are modelled by two stiffnesses with linear and nonlinear (cubic) parts. The friction coefficient μ at the contact is assumed to be constant as well as the velocity of the band. The relative velocity between the band and the velocities $\dot{X}_1$ and $\dot{X}_2$ is assumed positive which makes constant the direction of the friction force. According to the Coulomb's law, the tangential force F_{T} is assumed proportional to the normal force F_{N} that is: $F_{\mathrm{T}} = \mu F_{\mathrm{N}}$, see ([34, 36, 13]) for more details. The second order differential equation governing the dynamic behaviour of the system can be expressed in the state space by considering the state vector

$$\boldsymbol{x} = \begin{bmatrix} x_1 \\ x_2 \\ x_3 \\ x_4 \end{bmatrix} = \begin{bmatrix} X_1 \\ \dot{X}_1 \\ X_2 \\ \dot{X}_2 \end{bmatrix}$$

, so that a system like (1) can be obtained with:

$$\boldsymbol{f}(\boldsymbol{x}) = \begin{bmatrix} x_2 \\ -w_1^2 x_1 - \eta_1 w_1 x_2 + \mu w_2^2 x_3 - \psi_1^{\mathrm{NL}} x_1^3 + \mu \psi_2^{\mathrm{NL}} x_3^3 \\ x_4 \\ -\mu w_1^2 x_1 - w_2^2 x_3 - \eta_2 w_2 x_4 - \mu \psi_1^{\mathrm{NL}} x_1^3 - \psi_2^{\mathrm{NL}} x_3^3 \end{bmatrix}$$

while $\boldsymbol{g}(\boldsymbol{x})$ is taken equal to a constant column vector:

$$\boldsymbol{g}(\boldsymbol{x}) = \begin{bmatrix} 0 \\ 0 \\ 0 \\ 1 \end{bmatrix}$$

and $y = h(\boldsymbol{x}) = x_2$. The previous column vector defines the control matrix and indicates through the elements 1 or 0 the positions where the control input u is received. Otherwise, $w_i = \sqrt{k_i/m}$ are natural pulsations, $\eta_i = c_i/\sqrt{mk_i}$ are the relative damping and $\psi_i^{\mathrm{NL}} = k_i^{\mathrm{NL}}$, for $i = 1, 2$. For numerical simulation, all magnitudes are given in the MKSA (Meter (m), Kilograme (Kg), Second, Ampere) International System by: $w_1 = 2\pi \times 100$ rad/second, $w_2 = 2\pi \times 75$ rad/Second, $\eta_1 = \eta_2 = 0.02$, $\psi_1^{\mathrm{NL}} = w_1^2$, $\psi_2^{\mathrm{NL}} = 0$, $\mu = 0.4$ and $m = 1$ Kg.

4.1. Stability property and nonlinear dynamic behaviour

First, it can be verified that $(\boldsymbol{x_e}, u_e) = (\boldsymbol{0}, 0)$ is the solution of the nonlinear static equation corresponding to the Hultèn system and thus represents the system'equilibrium. The local stability of this equilibrium can be analysed by using the indirect Lyapunov method which is based on the analysis of the eigenvalues of the linearized system around the equilibrium [26]. Hence, $\boldsymbol{x}_e$ is said to be asymptotically stable if all the eigenvalues are with strictly negative real parts and unstable if at least one eigenvalue is with a positive real part. Results on the parametric stability analysis of the Hultèn system can be find in [38].

For the given set of parameter, the system presents two couples of complex conjugate eigenvalues that are plotted in Figure (2). The presence of eigenvalues in the right hand of the complex plan proofs the instability of the origin. Consequently, when the system state is moved from its equilibrium at $t = 0$ Second (for example $x_1(0) = 0.001$ m while the other states are kept at zero) then the system moves far away its equilibrium with

a divergence rate defined by the real parts of the unstable eigenvalues. The temporal evolutions of the displacement x_1 and the corresponding velocity x_2 that are obtained from the time integration of the nonlinear differential equations are plotted in Figures (3-a) and (3-b). The simulation time is fixed to $t_f = 3$ Seconds and is shown to be sufficient to reach stationary regime. The illustrated behaviour shows transient oscillations after it converges to periodic oscillating regime with a period $t_{\mathrm{p}} = 10^{-2}$ Sec and stationary amplitudes (0.563 m for the displacement x_1 and 310.7 m/Second for the velocity x_2. The same observation can be made about the displacement x_3 and the corresponding velocity x_4 which also converge to periodic oscillating regime with the same period $t_{\mathrm{p}} = 10^{-2}$ Second and stationary amplitudes (0.95 m and 547 m/Second, respectively). The observed behaviour represents the well known limit cycle phenomenon which can be recognized by isolated and closed curves in the phase plane. These are is illustrated in Figure (4-a) and Figure (4-b) where the velocities x_2 and x_4 are plotted against the displacements x_1 and x_3 respectively. As previously presented in the introduction, this friction-induced oscillations are undesirable and need to be suppressed or at least mitigated. Hence, we investigate in the following subsections the performances of the proposed nonlinear control techniques based on the feedback linearization principle.

[Figure 2 about here.]

[Figure 3 about here.]

[Figure 4 about here.]

4.2. Implementing of the input-state linearizing and stabilizing feedback

As presented in Section 3, the main step is to built a nonlinear coordinate transformation $\mathbf{\Phi}$ which permits the simplifying of the algebraic nonlinearities in the Hultèn model so that linear control techniques can be applied for the controlling of the friction-induced LCO. For this aim, the system needs to be input-state linearizable. The output function φ for which the system is input-state linearizable exists if the rank and involutivity conditions (1) and (2) given in Section 3, are fulfilled.

The matrix $\boldsymbol{M_g}$ associated to the nonlinear state representation of the Hultèn model is obtained as follows:

$$\boldsymbol{M}_g = \begin{bmatrix} 0 & 0 & 0 & -\mu w_2^2 \\ 0 & 0 & \mu w_2^2 & \eta_2 \mu w_2^3 + \eta_1 \mu w_1 w_2^2 \\ 0 & -1 & -\eta_2 w_2 & -\eta_2^2 w_2^2 + w_2^2 \\ 1 & \eta_2 w_2 & \eta_2^2 w_2^2 - w_2^2 & -\eta_2 w_2^3 - \eta_2 w_2 \left(-\eta_2^2 w_2^2 + w_2^2\right) \end{bmatrix} \tag{18}$$

It can be verified that $\boldsymbol{M}_g$ is a full rank matrix which satisfies the rank condition 1 . Otherwise, the distribution defined by $\bar{\Delta} = span\left\{\boldsymbol{g}, ad_{\boldsymbol{f}}\boldsymbol{g}, ad_{\boldsymbol{f}}^2\boldsymbol{g}\right\}$ is involutive according to the condition given in Definition 1. Ultimately, the rank and involutivity conditions (1) and (2) being fulfilled, the existence of the scalar output function φ ensuring the input-state linearization of the system can be confirmed.

By considering the displacement $\varphi(\boldsymbol{x}) = x_1$ as the output function, it can be verified that the relative degree r of the corresponding input/output relation equals 4 since we have:

$$\begin{cases} L_{\boldsymbol{g}} L_{\boldsymbol{f}}^k \varphi(\boldsymbol{x}) = 0 \quad k \in 0, 1, 2 \\ L_{\boldsymbol{g}} L_{\boldsymbol{f}}^3 \varphi(\boldsymbol{x}) = \mu w_2 \neq 0 \quad \forall \boldsymbol{x} \in R^4 \end{cases} \tag{19}$$

The relative degree $r = 4$ being equal to the system dimension, indicates that a full input-state linearization is possible for the system with the defined output function $\varphi(\boldsymbol{x}) = x_1$. The nonlinear coordinate transformation $\boldsymbol{z} = \boldsymbol{\Phi}(\boldsymbol{x})$ ensuring the input-state linearization of the Hultèn system is then given in accordance with expression (15) by:

$$\begin{cases} z_1 = x_1 \\ z_2 = x_2 \\ z_3 = -w_1^2 x_1 - \eta_1 w_1 x_2 + \mu w_2^2 x_3 - \psi_1^{\mathrm{NL}} x_1^3 \\ z_4 = \eta_1 w_1^3 x_1 + \left(\eta_1^2 w_1^2 - w_1^2\right) x_2 - \eta_1 w_1 w_2^2 \mu x_3 + \mu w_2^2 x_4 + \eta_1 w_1 \psi_1^{\mathrm{NL}} x_1^3 - 3\psi_1^{\mathrm{NL}} x_2 x_1^2 \end{cases} \tag{20}$$

In an equivalent way, the inverse transformation is obtained as follows:

$$\begin{cases} x_1 = z_1 \\ x_2 = z_2 \\ x_3 = \frac{1}{\mu w_2^2}\left(w_1^2 z_1 + \eta_1 w_1 z_2 + z_3 + \psi_1^{\mathrm{NL}} z_1^3\right) \\ x_4 = \frac{1}{\mu w_2^2}\left(w_1^2 z_2 + \eta_1 w_1 z_3 + z_4 + 3\psi_1^{\mathrm{NL}} z_1^2 z_2\right) \end{cases} \tag{21}$$

The linearizing control feedback is then determined by using the expression (16) and obtained as follows:

$$u = \frac{1}{\mu w_2^2} \begin{cases} -(x_2(\eta_1 w_1(w_1^2 + 3\psi_1 x_1^2) - 6\psi_1 x_1 x_2) + \\ (-\eta_1^2 w_1^2 + w_1^2 + 3\psi_1 x_1^2)(w_1^2 x_1 + \eta_1 x_2 w_1 - \mu x_3 w_2^2 + \psi_1 x_1^3) \\ -\mu w_2^2(\mu w_1^2 x_1 + x_3 w_2^2 + \eta_2 x_4 w_2 + \mu\psi_1 x_1^3) - \eta_1 \mu w_1 w_2^2 x_4) + v \end{cases} \tag{22}$$

In fact, all state variables and thus the state-feedback control can be written as functions in the considered output function $y = x_1$ and its successive derivatives. This proofs the flatness property of the considered Hultèn system with the associated output function $\varphi(\boldsymbol{x})$. In practice, the flatness property is equivalent to the input-state linearisability in the case of SISO systems [28].

$$\begin{cases} x_1 = y \\ x_2 = \dot{y} \\ x_3 = \frac{1}{\mu w_2^2}\left(w_1^2 y + \eta_1 w_1 \dot{y} + \ddot{y} + \psi_1^{\mathrm{NL}} y^3\right) \\ x_4 = \frac{1}{\mu w_2^2}\left(w_1^2 \dot{y} + \eta_1 w_1 \ddot{y} + z_4 + 3\psi_1^{\mathrm{NL}} y^2 \dot{y}\right) \end{cases} \tag{23}$$

With the new coordinates and by applying the corresponding linearizing feedback, a fourth order Brunovsky from as given by (17) is obtained. The stabilizing state feedback can be expressed by using the new coordinates z_i

$$v = -k_0 z_1 - k_1 z_2 - k_2 z_3 - k_3 z_4 \tag{24}$$

so the closed loop state matrix is obtained:

$$\boldsymbol{A}_{\mathrm{CL}} = \begin{bmatrix} 0 & 1 & 0 & 0 \\ 0 & 0 & 1 & 0 \\ 0 & 0 & 0 & 1 \\ -k_0 & -k_1 & -k_2 & -k_3 \end{bmatrix}$$

The making asymptotically stable of the closed loop system boils down to the calculating of the coefficients $k_i, i = 0, ..., 3$ such that the zeros of the characteristic polynomial $P(\lambda)$, which are the eigenvalues of the closed loop state matrix $\boldsymbol{A}_{\mathrm{CL}}$ are with strictly negative real parts.

$$P(\lambda) = k_0 + k_1\lambda + k_2\lambda^2 + k_3\lambda^3 + \lambda^4 \tag{25}$$

The eigenvalues are fixed according to the stability properties and thus to the dynamical behaviour desired for the controlled system. As shown previously, the uncontrolled Hultèn system presents periodic oscillations with stationary amplitudes that are needed to be suppressed or at least mitigated. For these perspectives, three different cases in terms of the location of the desired eigenvalues, are considered. The corresponding eigenvalues are plotted in Figure (5) together with the eigenvalues of the original unstable system. The eigenvalues of the closed loop system are assigned to locations with different distances from the imaginary axis which defines the stability/instability boundary. The first case (represented by rounds in Figure (5)) considers stable eigenvalues but very closed to the imaginary axis.Then, these are slightly shifted to the left of the imaginary axis for the second case (eigenvalues with squares) and clearly assigned far from the imaginary axis for the third case (eigenvalues with diamond). The temporal evolutions of the displacements x_1 and x_3 and the associated velocities x_2 and x_4 that are obtained from the time integration of the closed loop system, are plotted for each case in Figures (6),(7) and (8) respectively.

[Figure 5 about here.]

[Figure 6 about here.]

[Figure 7 about here.]

[Figure 8 about here.]

Different dynamical behaviours of the closed loop system are observed depending on the considered cases. This is in accordance with what can be expected since each case presents its own stability properties. From Figure (6) corresponding to the first case, the stationary oscillating regime initially observed for the uncontrolled Hultèn system is drastically modified. Indeed, the displacements x_1 and x_3 as well as the corresponding velocities x_2 and x_4 present oscillations with strongly mitigated amplitudes in comparison with the initial amplitudes. In fact, the oscillations observed for the controlled displacements are not stationary but correspond to transient regimes. The time simulation ($t_{\text{final}} = 3$) Seconds which was previously shown to be sufficient to reach stationary regimes characterized by LCO (periodic oscillations with constant amplitudes), is kept

unchanged for simulating the dynamic behaviour of the controlled system. Until this time, the system's displacements and velocities present oscillations the amplitudes of which are decaying with rates that are not important enough to permit fast convergence to the equilibrium, the decaying rates being defined by the real parts of the eigenvalues closely to the imaginary axis (as shown in Figure (5)). The dynamic oscillations are consequently weakly damped and a small perturbation of the system equilibrium will make the controlled system oscillate for a longer time before it asymptotically converges to the equilibrium. The controlled displacement x_1 and velocity x_2 obtained from the time integration of the closed loop system with $t_f = 10$ Seconds, are plotted in Figure (9). The asymptotic stability of the closed loop system is clearly observed but with slow convergence properties.

[Figure 9 about here.]

The shifting of the eigenvalues of the closed loop system to the left permits to augment the decaying rates of the amplitude of oscillations and thus to accelerate the convergence to the equilibrium after the perturbation. Indeed, in Figure (7), it can be observed that the friction-induced oscillations shown by the uncontrolled system are suppressed. The transient regimes are shorter than those observed in the first case. Indeed, the displacements x_1 and x_3 and the associated velocities x_2 and x_4 converge asymptotically and more rapidly to the equilibrium (almost from $t = 1.3$ Seconds). In fact, the linearizing and stabilizing feedback has a friction-compensation effect which can be symbolically seen as a decrease of the value of the friction coefficient . The plot of x_1 and x_2 corresponding to the Hultèn's system with $\mu = 0.15$ in Figure (11) are in a perfect accordance with those corresponding to the controlled system in the second case. Concretely, the applied nonlinear state feedback has moved the initial unstable system away from the mode-coupling zone around which the equilibrium has already lost its asymptotic stability (see Figure (10)). The mode-coupling zone is characterized by the coalescence point ($\mu_c \approx 0.289$ for the considered system) near which the imaginary parts (and thus the frequencies) of the system, become equal while the corresponding real parts separate. One of the eigenvalues becoming positive will make unstable the equilibrium and its small perturbation will potentially put the system into an oscillatory regime. In an equivalent

way, by placing a couple of eigenvalues (as in the first case) at locations very closed to the imaginary axis, in fact this operation has brought the system close to the coalescence zone of the system modes while the linearizing and stabilizing state feedback determined in the second case, has permitted to the system to move further far the coalescence zone. The distance from the coalescence zone can be much marked by assigning the eigenvalues to values that are further to left. This is considered in the third case where two eigenvalues have been assigned to higher strict negative real parts while the others have been kept complex conjugate with negative real parts. The dynamic behaviour of the closed loop system illustrated in Figure (8) show better stability properties (faster transient with smaller amplitudes). The friction-induced LCO is suppressed and the displayed behaviour clearly shows the asymptotic stability of the closed loop system. After a few number of oscillations with small amplitudes (in comparison with the LCO amplitudes), the displacements x_1 and x_3 as well as the associated velocities converge quickly to the origin (from $t \approx 0.4$ second for all the magnitudes).

[Figure 10 about here.]

[Figure 11 about here.]

4.3. Implementing the input/output linearizing and stabilizing feedback

In the previous subsection, a complete linearizing state feedback has been determined after the obtaining of a fictive output function $\varphi(\boldsymbol{x})$ satisfying the rank and involutive conditions. In the general case, finding a such output function which in addition should have a relative degree equal to the system's dimension, is not a trivial task. In numerous cases, only output functions with relative degrees $r < n$ are more easily obtained. In a such case, as previously presented in Subsection 3.1, only a partial linearization is possible and an input-output linearization can be ensured instead of the complete input-state linearization. However, the stabilization of the partially linearized closed loop system is submitted to the stability condition of the zero-dynamics which is uncontrollable.

The output function of the Hultèn system is given by $y = h(\boldsymbol{x}) = x_2$, it can be verified that the corresponding relative degree is equal to $r = 3$ which is smaller than $n = 4$. Hence, only a partial linearization is possible. In this perspective the following nonlinear

coordinates must be completed in accordance to the equations (7) and (8), to form the diffeomorphism:

$$\begin{cases} z_1 = x_2 \\ z_2 = -w1^2 x_1 - \eta_1 x_2 w_1 + \mu w2^2 x_3 - \psi_1^{\mathrm{NL}} x_1^3 \\ z_3 = \mu w_2^2 x_4 - x_2(w_1^2 + 3\psi_1^{\mathrm{NL}} x_1^2) + \eta_1 w_1(w_1^2 x_1 + \eta_1 x_2 w_1 - \mu x_3 w_2^2 + \psi_1^{\mathrm{NL}} x_1^3) \end{cases} \tag{26}$$

The remaining coordinate $z_4 = \phi_4(\boldsymbol{x}) = x_1$ can be considered since it is a solution of equation (8). So, by applying the completed nonlinear coordinate transformation and the state feedback corresponding to (9) with (10), the following closed loop system is obtained:

$$\begin{cases} \dot{z}_1 = z_2 \\ \dot{z}_2 = z_3 \\ \quad \vdots \\ \dot{z}_3 = v \\ \dot{z}_4 = z_1 \end{cases} \tag{27}$$

The eigenvalues of the linear controllable part in (27) are assigned to values in the left half complex plan in order to guaranty its asymptotic stability. Their locations are illustrated in Figure (12). Then, the obtained closed loop system is excited by applying a small perturbation on the displacement; $x_1 = 0.001$ m. The temporal evolutions of the displacements x_1 and x_3 and the associated velocities x_2 and x_4 obtained from the time integration of the corresponding differential equations are illustrated in Figure (13).

[Figure 12 about here.]

It can be observed that the friction-induced LCO are completely suppressed after some transient oscillations. The displacements x_1 and x_3 and the corresponding velocities x_2 and x_4 have converged to stationary regimes that are devoid of any oscillation. This confirms the stable behaviour of the closed loop system. Note that, assigning the eigenvalues to further to left in the complex plane permits to shorten the transient regimes of the observed magnitudes, as in the previous studied case about the input-state linearizing feedback. The same interpretation about the the friction-compensation effect for the stabilizing state feedback previously given, can be also stated in this case. However, it can be remarked that x_1 and x_3 have reached -0.06 m and -0.24 m as final values

respectively. This shows that the stability of the equilibrium of the controlled system is not asymptotic. This is due to the zero-dynamics, $\dot{z}_4 = 0$, associated to the obtained closed loop system obtained. Indeed, the zero-dynamics corresponds to a pure integrator system which is known to be a stable but not asymptotically stable system. Hence, the equilibrium of the whole closed loop is only stable.

[Figure 13 about here.]

Remark: In fact, in the presented study, the contact is assumed to be maintained during the vibration. Other studies have considered the opposite case as in [39] for slider-belt system. In this case namely in the situations when the contact may be lost and/or stick-slip vibration may occur, the feedback linearizing techniques such presented in this study become inefficient anf even unsuitable. Indeed, smoothness and derivability properties are required for the effectiveness of the proposed approach.

5. Conclusion

This study has presented nonlinear schemes for the active control of nonlinear dynamical friction systems submitted to mode-coupling instabilities. The proposed schemes are based on the feedback linearization principle. The effectiveness of the proposed has been shown by considering an academic system which is well recognized as a suitable benchmark for representing mode-coupling instabilities occurring in brake systems. The proposed nonlinear control techniques have permitted the suppressing of the friction-induced LCO. Otherwise, it is necessary to observe that the implementing of feedback linearizing approach considers that the system's degrees of freedom are measurable which is not necessary the case in practice. In this situation, the use of state observer becomes necessary. Otherwise, the linearizing feedback based approaches presented in this study are unsuitable when the non-linearities are non-regular. Moreover, they are sensitive to parameter uncertainty and/or unmodeled dynamics so no robustness is guaranteed.In addition, for practical implementation, the control inputs are always subjected to the saturation problem. All these issues associated to high dimensional friction systems are research in progress.

6. References

[1] N. M. Kindkaid, O. M. O'Reilly, and P. Papadopoulos. Automative disc brake squeal. *Journal of Sound and Vibration*, 267:105–166, 2003.

[2] H. Ouyang, W. Nack, Y. Yuan, and F. Chen. Numerical analysis of automative disc brake squeal: a review. *International Journal of Vehicle Noise and Vibration*, 1:207–231, 2005.

[3] R.A. Ibrahim. Friction-induced vibration, chatter, squeal, and chaos part 1: mechanics of contact and friction. *Am Soc Mech Eng Appl Mech Rev*, 47(7):209–226, 1994.

[4] R.A. Ibrahim. Friction-induced vibration, chatter, squeal, and chaos part 2: dynamics and modeling. *Am Soc Mech Eng Appl Mech Rev*, 47(7):227–263, 1994.

[5] A.R. AbuBakar and H. Ouyang. Complex eigenvalue analysis and dynamic transient analysis in predicting disc brake squeal. *International Journal of Vehicle Noise and Vibration*, 2:143–155, 2006.

[6] A.R. AbuBakar and H. Ouyang. A prediction methodology of disk brake squeal using complex eigenvalue analysis. *International Journal of Vehicle Design*, 46(4):416–435, 2008.

[7] J.-J. Sinou and S. Besset. Simulation of transient nonlinear friction-induced vibrations using complex interface modes: Application to the prediction of squeal events. *Shock and Vibration*, 2017, 2017. 10 pages.

[8] N. Hoffmann and L. Gaul. Effects of damping on mode-coupling instability in friction induced oscillations. *ZAMM - Journal of Applied Mathematics and Mechanics*, 83(8):524–534, 2003.

[9] T. Bultin and J. Woodhouse. Friction-induced vibration: quantifying sensitivity and uncertainty. *Journal of Sound and Vibration*, 329(1-2):509–526, 2010.

[10] S. Oberst and J.C.S. Lai. Statistical analysis of brake squeal noise. *Journal of Sound and Vibration*, 330(12):2978–2994, 2011.

[11] L. Nechak, S. Berger, and E. Aubry. Prediction of random self friction-induced vibrations in uncertain dry friction systems using a multi-element generalized polynomial chaos approach. *Journal of Vibration and Acoustics*, 134(4):14, 2012.

[12] L. Nechak, S. Berger, and E. Aubry. Wiener haar expansion for the modeling and prediction of the dynamic behavior of self-excited nonlinear uncertain systems. *ASME Journal of Dynamic Systems, Measurement, and Control*, 134(5):051011, 2012.

[13] E. Sarrouy, O. Dessombz, and J.-J. Sinou. Stochastic study of non-linear self-excited system with friction. *European Journal of Mechanics A/Solids*, 40(2):1–10, 2013.

[14] A. Nobari, H. Ouyang, and P. Bannister. Statistics of complex eigenvalues in friction-induced vibration. *Journal of Sound and Vibration*, 338:169–183, 2015.

[15] B. Bergeot, S. Berger, and S. Bellizzi. Mode coupling instability mitigation in friction systems by means of nonlinear energy sinks: numerical ighlighting and local stability analysis. *Journal of Vibration and Control*, 24(15):3487–3511, 2017.

[16] K. Popp and M. Rudolph. Vibration control to avoid stick-slip motion. *Journal of Vibration and Control*, 10:1585–1600, 2004.

[17] H. Ouyang. Prediction and assignment of latent roots of damped asymmetric systems by structural modifications. *Mechanical Systems and Signal Processing*, 23(6):1920–1930, 2009.

[18] H. Ouyang. Pole assignment of vriction-induced vibration for stabilisation through state-feedback control. *Journal of Sound and Vibration*, 329(11):1985–1991, 2009.

[19] K. V. Singh and H. Ouyang. Pole assignment using state feedback with time delay in friction-induced vibration problems. *Acta Mechanica*, 224(3):645–656, 2012.

[20] A. Saha, B. Bhattacharya, and P. Wahi. A comparitive study on the control of friction-driven oscillations by time- delayed feedback. *Nonlinear Dynamics*, 60:15–37, 2010.

[21] J. Das and A. K. Mallik. Control of friction driven oscillation by time-delayed state feedback. *Journal of Sound and Vibration*, 297(3-5):578–594, 2006.

[22] S. Chatterjee. Time-delayed feedback control of friction-induced instability. *International Journal of Nonlinear Mechanics*, 42:1143–1127, 2007.

[23] M. G. Tehrani and H. Ouyang. Receptance-based partial pole assignment for asymmetric systems using state-feedback. *Shock and Vibration*, 19(5):1135–1142, 2012.

[24] Y. Liang, H. Yamaura, and H. Ouyang. Active assignment of eigenvalues and eigen-sensitivities for robust stabilization of friction-induced vibration. *Mechanical Systems and Signal Processing*, 90:254–267, 2017.

[25] N. Sun, T. Yang, Y. Fang, and Y. Wu. Transportation control of double-pendulum cranes with a nonlinear quasi-pid scheme: design and experiments. *IEEE Transactions on Systems, Man, and Cybernetics*, 99:1–11, 2018.

[26] H. Khalil. *Nonlinear Systems*. Prentice Hall, 2002.

[27] J-J. Slotine and L. Weiping. *Applied Nonlinear Control*. Prentice Hall, 1991.

[28] M. Fliess, M. Levine, J. Martin, and P. Rouchon. Flatness and defect of nonlinear systems:introductory theory and examples. *International Journal of Control*, 61:645–656, 2012.

[29] T. Kailath. *Linear Systems*. Prentice Hall, 1980.

[30] T. J. Koo and S. Sastry. Output tracking control design of a helicopter model based on approximate linearization. In *In the Proceedings of the 37th IEEE Conference on Decision and Control*, page 10.1109/CDC.1998.761745, 1998.

[31] D. D. Da Silva, W. L. Turcio, and E. A. Tannuri. Temperature control of an aeronautical pneumatic system using feedback linearization and pid. *Automatica*, 37:1845–1851, 2014.

[32] C. Chapuis, X. Brun, E. Bideaux, and N. Minoiu-Enache. Comparison of feedback linearization and flatness control for anti-slip regulation (asr) of an hybrid vehicle: From theory to experimental results. In *In the proceeding of 2013 European Conference on Control*, page DOI: 10.23919/ECC.2013.6669127, 2013.

[33] C. Zhen, S. Jiffri, D. Li, J. Xiang, and J. E. Mottershead. Feedback linearisation of nonlinear vibration problems: A new formulation by the method of receptances. *Mechanical Systems and Signal Processing*, 98:1056–1068, 2018.

[34] J. Hult èn. Drum brake squeal- a self exciting mechanism with constant friction. In *In the SAE truck and bus meeting, 1993, Detroit, MI, USA SAE paper*, page 932965, 1993.

[35] J-J. Sinou and L. Jézéquel. Mode coupling instability in friction-induced vibrations and its dependency on system parameters including damping. *European Journal of Mechanical A/Solid*, 26:107–122, 2007.

[36] J-J. Sinou, G. Fritz, and L. Jézéquel. The role of damping and definition of the robust damping factor for a self-exciting mechanism with constant friction. *Journal of vibration and acoustics*, 129:297–307, 2007.

[37] L. Nechak, S. Berger, and E. Aubry. A polynomial chaos approach to the robust analysis of the dynamic behaviour of friction systems. *European Journal of Mechanics A/Solids*, 30(4):594–607, 2011.

[38] L. Nechak, S. Berger, and E. Aubry. Non-intrusive generalized polynomial chaos for the stability analysis of uncertain dynamic friction systems. *Journal of Sound and Vibration*, 332(5):1204–1215, 2013.

[39] Z. Li, H. Ouyang, and Z. Guan. Nonlinear friction-induced vibration of a slider -belt system. *Journal of Vibration and Acoustics*, 138:DOI: 10.1115/1.4033256, 2016.

List of Figures

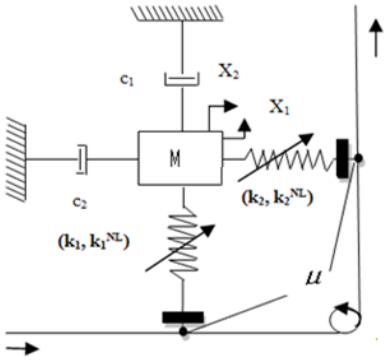

Figure 1: Mechanical system

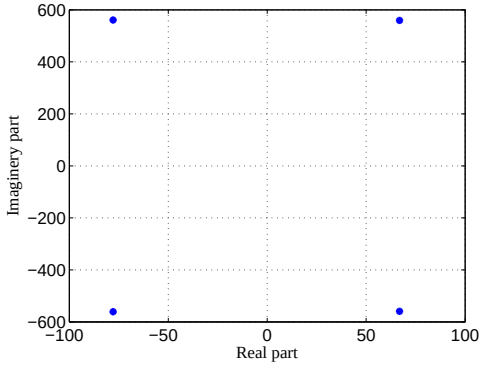

Figure 2: Eigenvalues of the linearized system arround $\boldsymbol{x}_e = (\mathbf{0}, 0)$

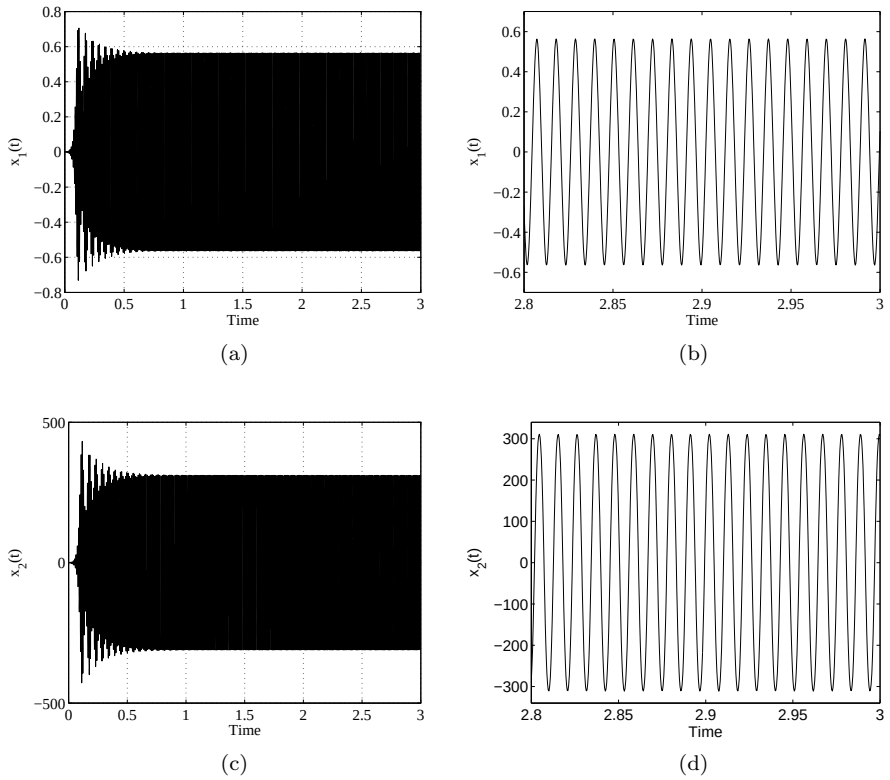

Figure 3: Temporal evolutions of: (a) the displacement $x_1(t)$ and (b) the velocity $x_2(t)$ versus time. (b) and (d) represent zooms on few periods of oscillations of $x_1(t)$ and $x_2(t)$ respectively

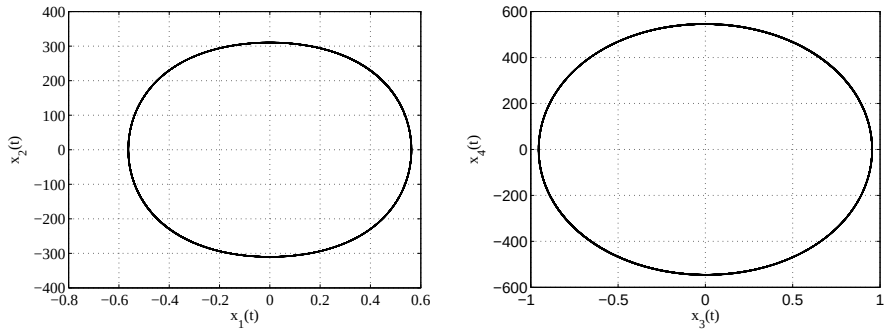

(a) (b)

Figure 4: Velocity versus the displacement: (a) $x_2(t)$ versus $x_1(t)$, (b) $x_4(t)$ versus $x_3(t)$

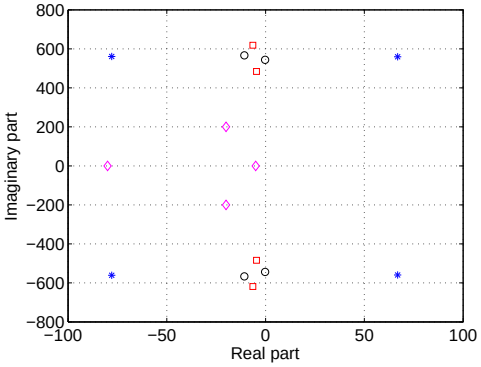

Figure 5: Location of the desired eigenvalues for the closed loop system

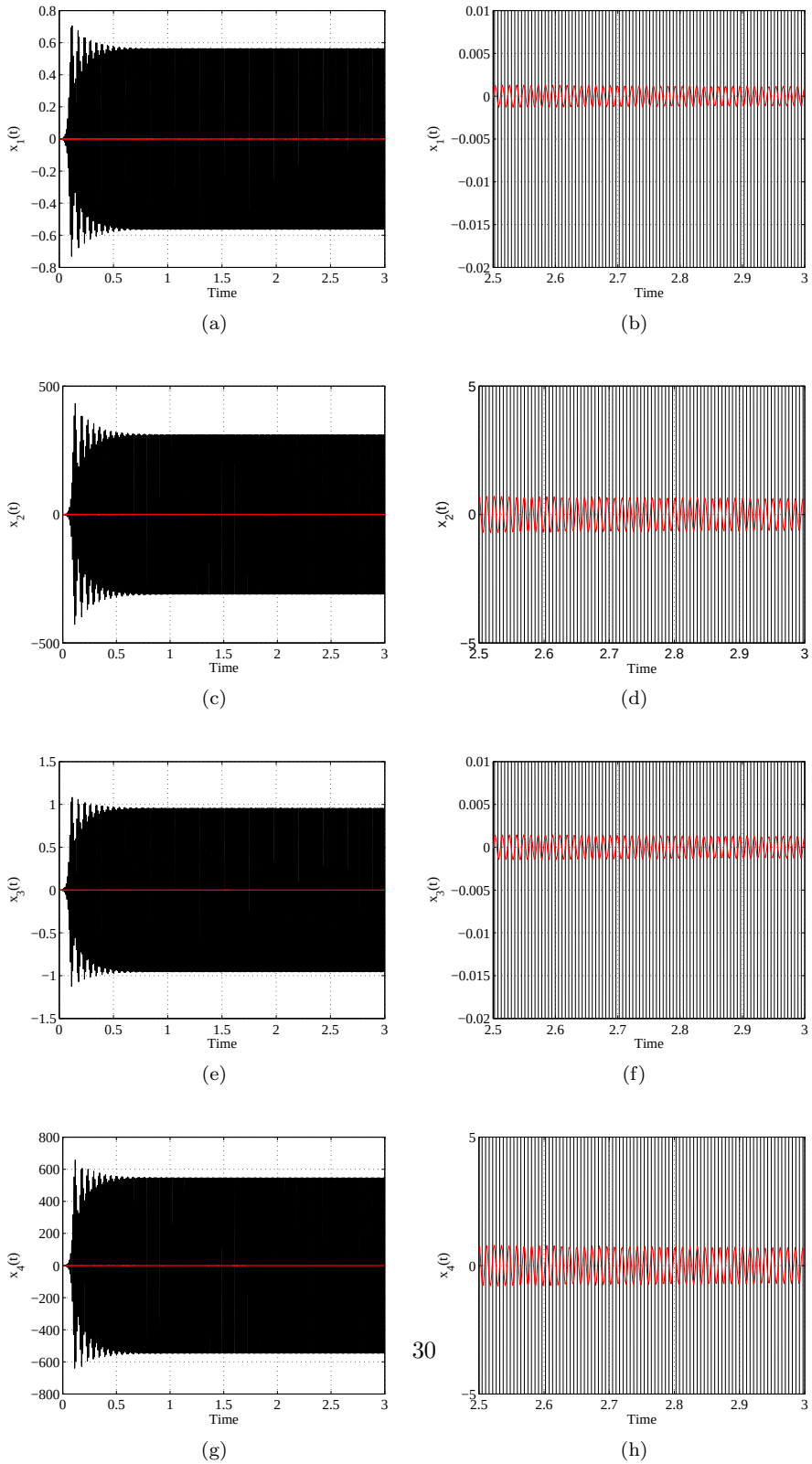

Figure 6: The temporal evolutions of: (a) the displacement $x_1(t)$, (c) the velocity $x_2(t)$, (e) the displacement $x_3(t)$ and (g) the velocity $x_4(t)$, versus time corresponding to the first case (eigenvalues close to the imaginary axis). (b), (d), (f) and (h) represent zooms on few periods of oscillations of $x_1(t)$, $x_2(t)$, $x_3(t)$ and $x_4(t)$, respectively. Dark line: original system, red line: closed loop system

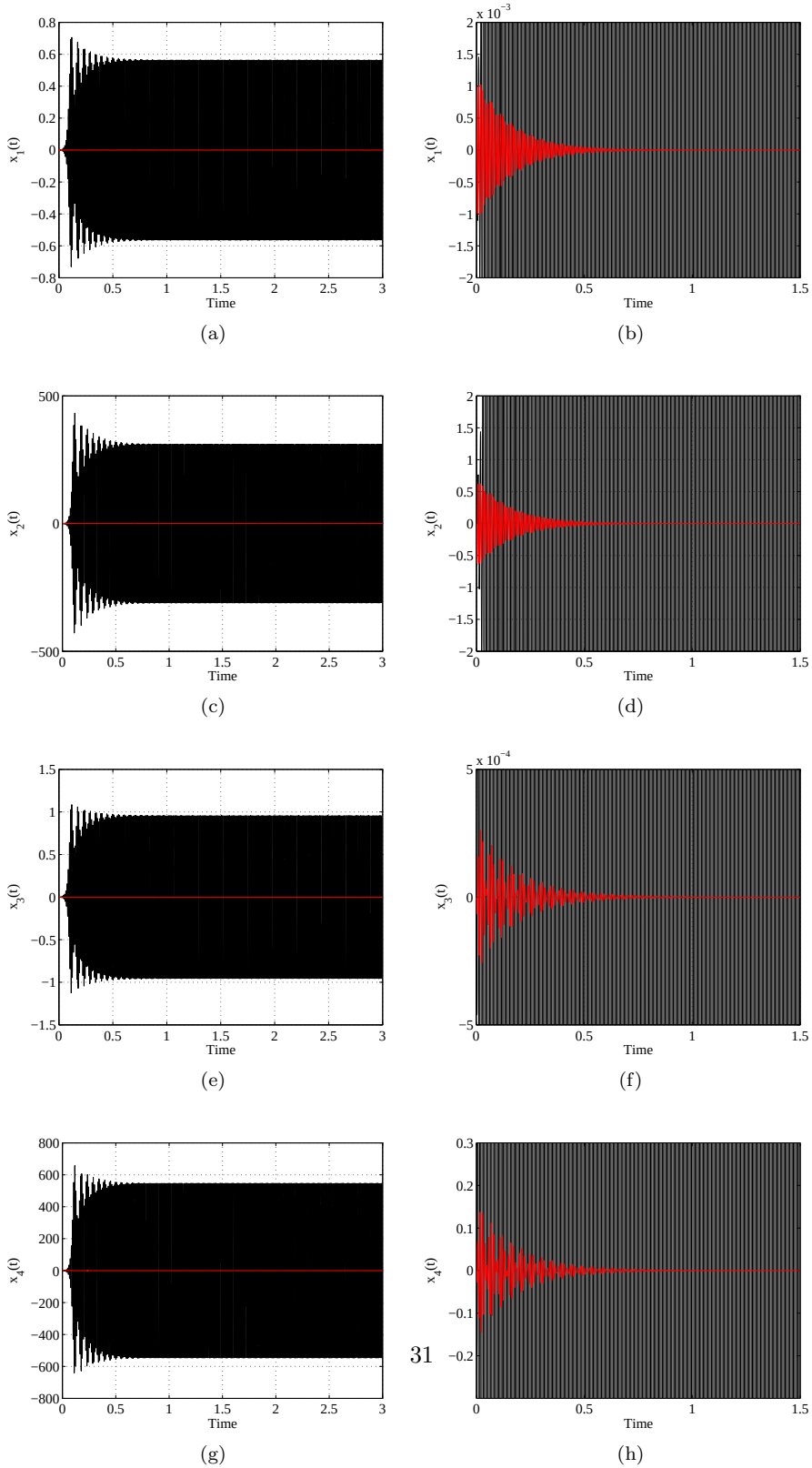

Figure 7: The temporal evolutions of: (a) the displacement $x_1(t)$, (c) the velocity $x_2(t)$, (e) the displacement $x_3(t)$ and (g) the velocity $x_4(t)$, versus time corresponding to the second case (eigenvalues shifted from the imaginary axis). (b), (d), (f) and (h) represent zooms on few periods of oscillations of $x_1(t)$, $x_2(t)$, $x_3(t)$ and $x_4(t)$, respectively. Dark line: original system, red line: closed loop system

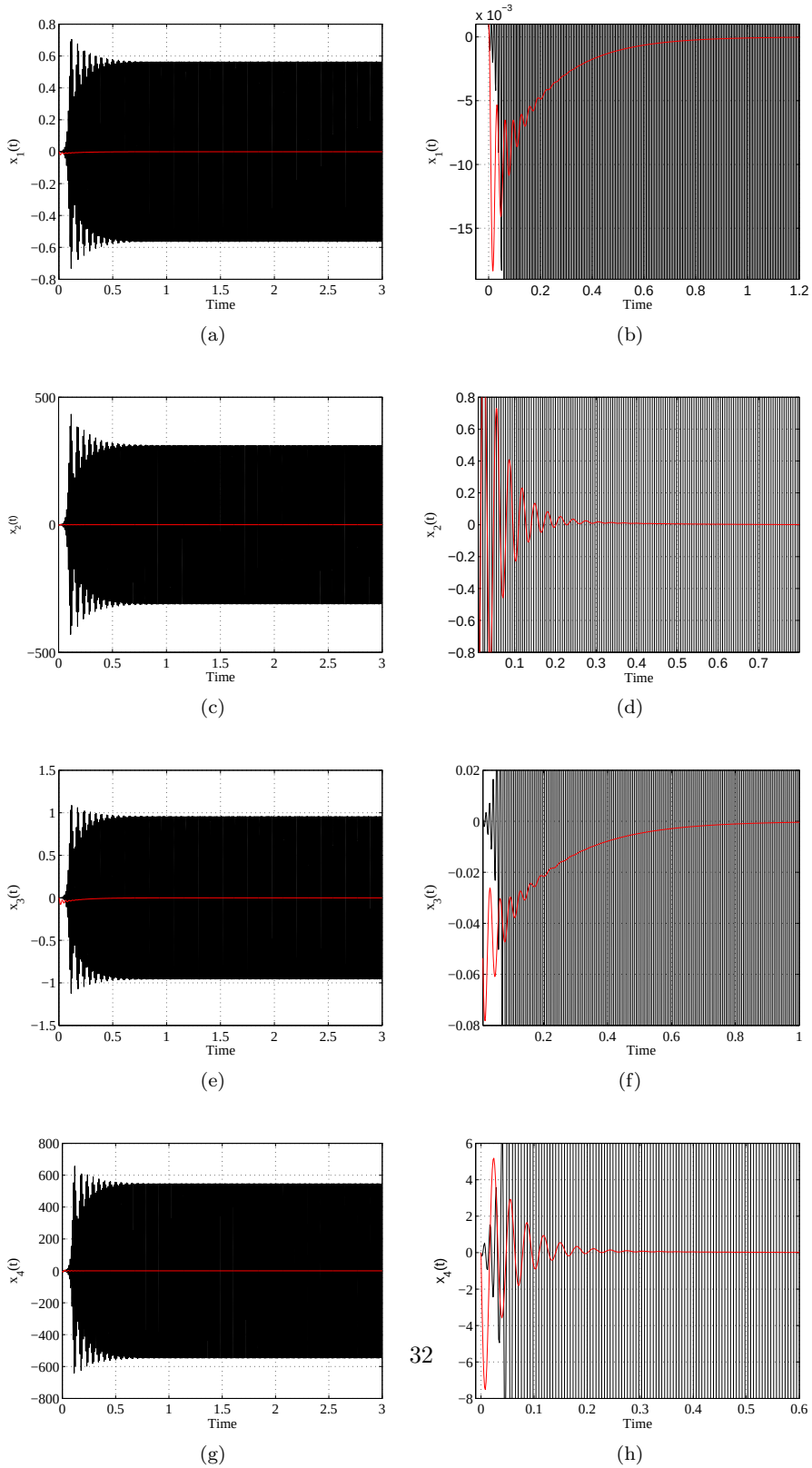

Figure 8: The temporal evolutions of: (a) the displacement $x_1(t)$, (c) the velocity $x_2(t)$, (e) the displacement $x_3(t)$ and (g) the velocity $x_4(t)$, versus time corresponding to the third case (eigenvalues far from the imaginary axis). (b), (d), (f) and (h) represent zooms on few periods of oscillations of $x_1(t)$, $x_2(t)$, $x_3(t)$ and $x_4(t)$, respectively. Dark line: original system, red line: closed loop system

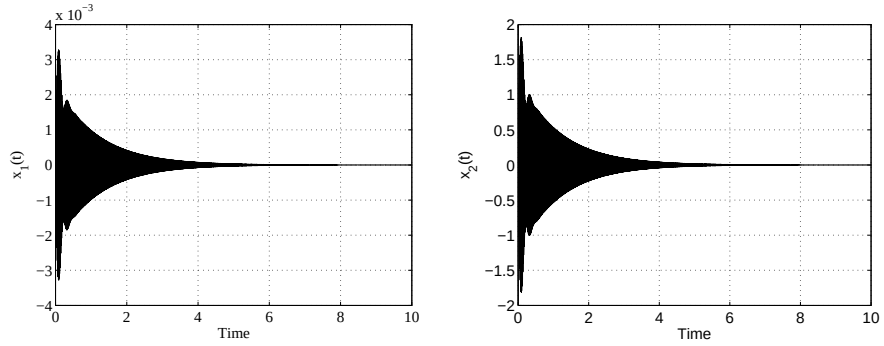

(a) (b)

Figure 9: Long time integration of the close loop system corresponding to the first case (eigenvalues close to the imaginary axis): (a) the displacement $x_1(t)$ and (b) the velocity $x_2(t)$

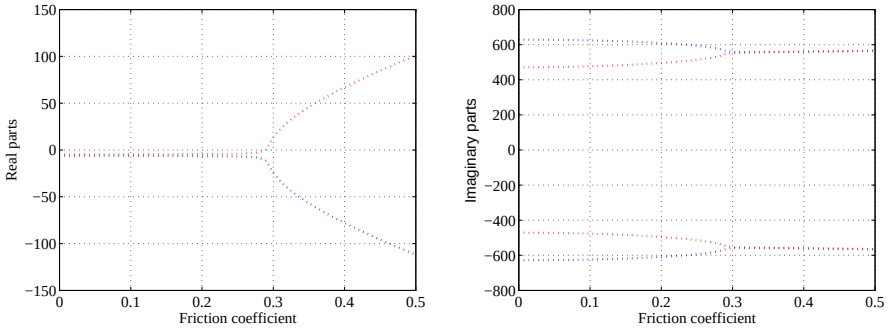

(a) (b)

Figure 10: Evolution of the eigenvalues of the Hultèn system linearized around the origin, versus the friction coefficient μ

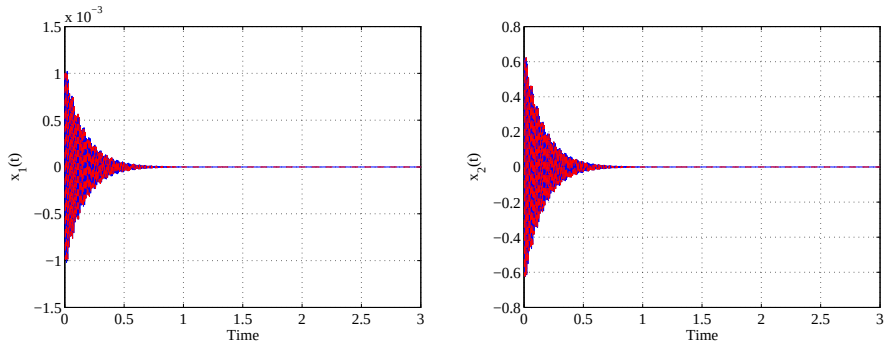

(a) (b)

Figure 11: The temporal evolution of the displacement $x_1(t)$ and the velocity $x_2(t)$ of the Hultèn system corresponding to $\mu = 0.15$ in comparison with those of the closed loop system. Blue line: original system, red line: closed loop system

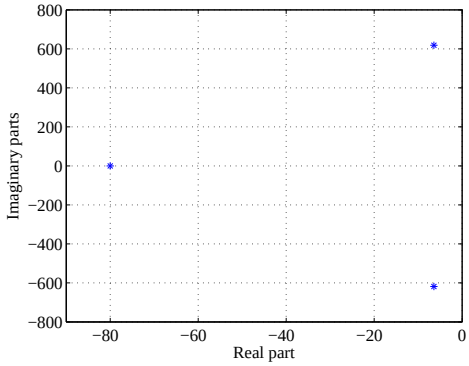

Figure 12: Location of the desired eigenvalues for the partially linearized system

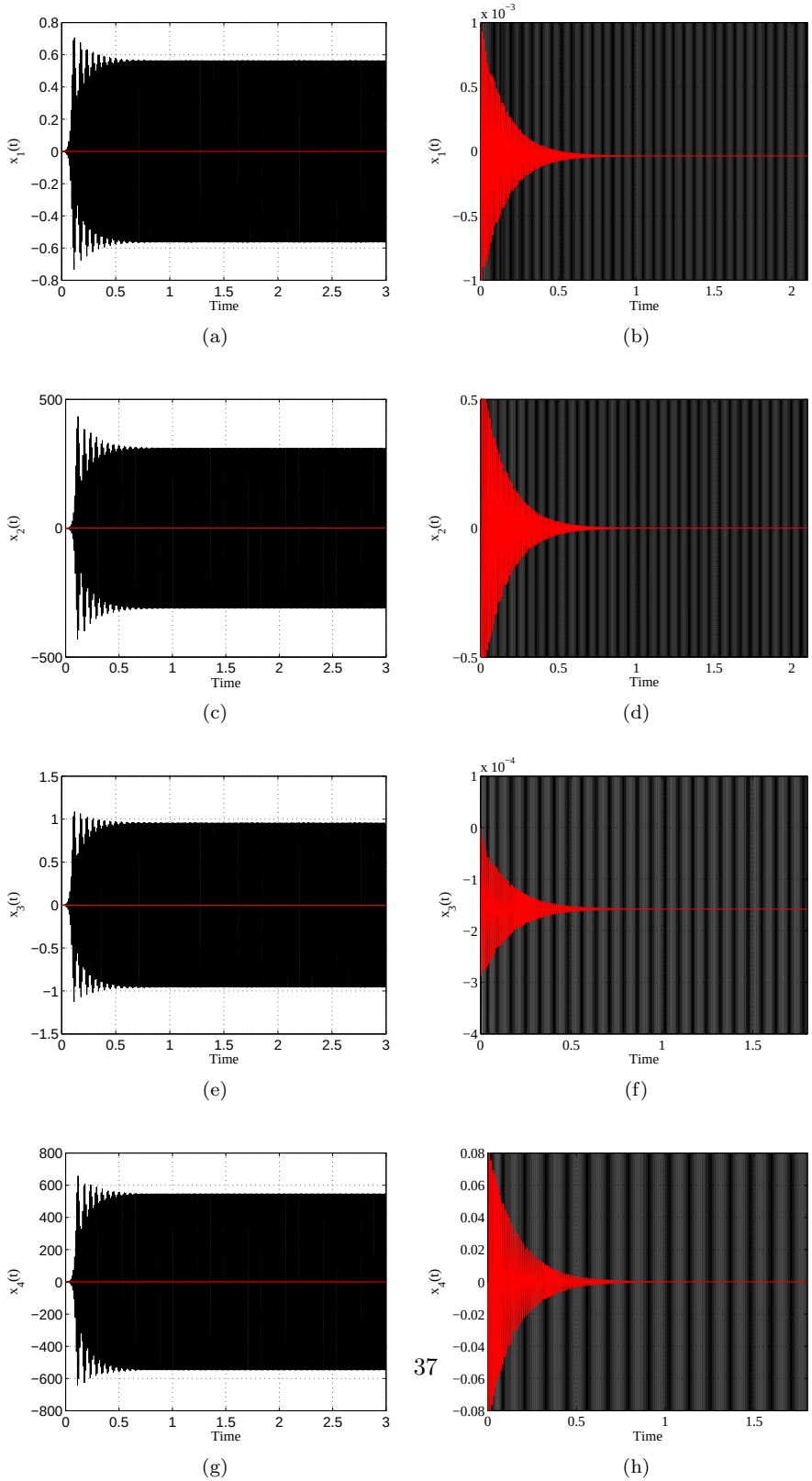

Figure 13: The temporal evolutions of: (a) the displacement $x_1(t)$, (c) the velocity $x_2(t)$, (e) the displacement $x_3(t)$ and (g) the velocity $x_4(t)$, versus time corresponding. (b), (d), (f) and (h) represent zooms on few periods of oscillations of $x_1(t)$, $x_2(t)$, $x_3(t)$ and $x_4(t)$, respectively. Dark line: original system, red line: Input-output linearized system